

Structural, electronic, and magnetic properties of quaternary Heusler CrZrCo*Z* compounds: A first-principles study

Xiao-Ping Wei(魏小平), Tie-Yi Cao(曹铁义), Xiao-Wei Sun(孙小伟), Qiang Gao(高强), Peifeng Gao(高配峰), Zhi-Lei Gao(高治磊), Xiao-Ma Tao(陶小马)

Citation: Chin. Phys. B . 2020, 29(7): 077105 . **doi:** 10.1088/1674-1056/ab969b
Journal homepage: http://cpb.iphy.ac.cn; http://iopscience.iop.org/cpb

What follows is a list of articles you may be interested in

Electronic properties of size-dependent $MoTe_2$/WTe_2 heterostructure

Jing Liu(刘婧), Ya-Qiang Ma(马亚强), Ya-Wei Dai(戴雅薇), Yang Chen(陈炀), Yi Li(李依), Ya-Nan Tang(唐亚楠), Xian-Qi Dai(戴宪起)

Chin. Phys. B . 2019, 28(10): 107101 . **doi:** 10.1088/1674-1056/ab3b53

Electronic structure from equivalent differential equations of Hartree-Fock equations

Hai Lin(林海)

Chin. Phys. B . 2019, 28(8): 087101 . **doi:** 10.1088/1674-1056/28/8/087101

First-principles study on the mechanics, optical, and phonon properties of carbon chains

Jin-Ping Li(李金平), Song-He Meng(孟松鹤), Han-Tao Lu(陆汉涛), Takami Tohyama(遠山貴巳)

Chin. Phys. B . 2018, 27(11): 117101 . **doi:** 10.1088/1674-1056/27/11/117101

First principles study of stability, mechanical, and electronic properties of chromium silicides

Bo Ren(任博), De-Hong Lu(卢德宏), Rong Zhou(周荣), De-Peng Ji(姬德朋), Ming-Yu Hu(胡明钰), Jing Feng(冯晶)

Chin. Phys. B . 2018, 27(10): 107102 . **doi:** 10.1088/1674-1056/27/10/107102

Effect of Mn doping on mechanical properties and electronic structure of WCoB ternary boride by first-principles calculations

Tong Zhang(张桐), Hai-Qing Yin(尹海清), Cong Zhang(张聪), Xuan-Hui Qu(曲选辉), Qing-Jun Zheng(郑清军)

Chin. Phys. B . 2018, 27(10): 107101 . **doi:** 10.1088/1674-1056/27/10/107101

Structural, electronic, and magnetic properties of quaternary Heusler CrZrCoZ compounds: A first-principles study*

Xiao-Ping Wei(魏小平)[1,†], Tie-Yi Cao(曹铁义)[1], Xiao-Wei Sun(孙小伟)[1], Qiang Gao(高强)[2], Peifeng Gao(高配峰)[3], Zhi-Lei Gao(高治磊)[1], and Xiao-Ma Tao(陶小马)[4]

[1] *The School of Mathematics and Physics, Lanzhou Jiaotong University, Lanzhou* 730070, *China*
[2] *Institute of Materials Science, Technische Universitat Darmstadt,* 64287 *Darmstadt, Germany*
[3] *Key Laboratory of Mechanics on Western Disaster and Environment, Ministry of Education, College of Civil Engineering and Mechanics, Key Laboratory of Special Function Materials and Structure Design of Ministry of Education, Lanzhou University, Lanzhou* 730000, *China*
[4] *School of Physical Science and Technology, Guangxi University, Nanning* 530004, *China*

(Received 23 March 2020; revised manuscript received 15 May 2020; accepted manuscript online 27 May 2020)

Using the first-principles calculations, we study the structural, electronic, and magnetic properties along with exchange interactions and Curie temperatures for CrZrCoZ (Z = Al, Ga, In, Tl, Si, Pb) quaternary Heusler alloys. The results show that the CrZrCoZ alloys are half-metallic ferrimagnets, and their total spin magnetic moments, which are mainly carried by the Cr atom, obey the Slater–Pauling rule. Analysis of local density of states confirms that the exchange splitting between e_g and t_{2g} states leads to the formation of half-metallic gap. According to the calculated Heisenberg exchange coupling parameters, it is found that the Cr(A)–Cr(A) and Cr(A)–Zr(B) exchanges dominate the appearance of ferrimagnetic states in CrZrCoZ (Z = Al, Ga, In, Tl, Pb) alloys, and it is the Cr(A)–Zr(B) and Zr(B)–Zr(B) exchanges for CrZrCoSi alloy. Finally, we estimate the Curie temperatures of CrZrCoZ by using mean-field approximation, it is found that the CrZrCoZ (Z = Al, Ga, In, Tl, Pb) alloys have noticeably higher Curie temperatures than room temperature. So, we expect that the CrZrCoZ alloys are promising candidates in spintronic applications in future.

Keywords: quaternary Heusler alloys, electronic structure, magnetic properties, Curie temperature

PACS: 71.20.Lp, 85.75.Dd, 75.50.–y, 77.80.B– **DOI:** 10.1088/1674-1056/ab969b

1. Introduction

Heusler alloys have attracted wide attention over the last decades because of their multi-functional properties, such as half-metallic magnetism,[1–5] magnetic shape memory behavior,[6–11] spin gapless semiconductor,[12–15] giant magnetocaloric effect,[16,17] thermoelectric effects,[18,19] superconductivity,[20] and so on, these properties succeed in technological applications. For example, the half-metallicity has been used in spin injectors, magnetic tunnel junctions, spin valves, and spin torque transfer-random access memories.[21]

Usually, Heusler alloys can be classified into half-Heusler and full-Heusler alloys, the former has a general chemical formula XYZ, and crystallizes into $C1_b$ structure with $F\bar{4}3m$ space group, where X and Y represent transition metals, and Z is of sp element; the latter has stoichiometry X_2YZ, and crystallizes into $L2_1$ structure with $Fm\bar{3}m$ space group.[22–24] By substituting another transition metal X' for X in full-Heusler alloys X_2YZ, the quaternary Heusler alloys $XX'YZ$ with LiMgPdSn prototype are formed.[25,26] The quaternary Heusler alloys have greater flexibilities on the choices of components and atomic arrangements, thus they may offer newer materials with target properties. So far, many quaternary Heusler alloys as spintronic candidates have been reported to be half-metallicity with high Curie temperature.[3,27–31]

Among these quaternary Heusler alloys, the Cr-based quaternary Heusler alloys, as a subset of these materials, have been studied extensively from the perspectives of theory and experiment.[13,32–40] For instance, it has been confirmed experimentally that the CoFeCrGe alloy crystalizes with LiMgPdSn structure, and has an integer magnetic moment of 3.0 μ_B/f.u. together with a Curie temperature of 866 K.[41] The CoFeCrZ (Z = P, As, Sb) and CoFeCrZ (Z = Al, Si, Ga, Ge) alloys were predicted to be half-metals.[27,42,43] From these reports, we notice that there are two magnetic atoms in these quaternary Heusler alloys, only a few studies focus on the quaternary Heusler alloys including one magnetic atom.[32,38,44,45] Therefore, it is necessary to design new quaternary Heusler alloys with half-metallicity to understand the effects of the presence of one magnetic atom. Apart from the quest, another motivation is to explore whether new half-metallic magnets with high Curie temperature can be derived from the family of Heusler alloys by changing the compositions and thus expand the database of materials for spintronic applications.

Up to now, the Cr_2CoZ (Z = Al, Ga, In, Si, Ge, Sn, Pb) alloys have been predicted to be half-metals with low magnetic moments.[46–48] Accordingly, the half-metallicity is also observed in Zr_2CoZ (Z = Al, Ga, In, Tl, Si, Ge, Sn, Pb)

*Project supported by the National Natural Science Foundation of China (Grant No. 11864021) and Foundation of A Hundred Youth Talents Training Program of Lanzhou Jiaotong University, China, the Key Talent Foundation of Gansu Province, China (Grant No. 2020RCXM100), and Excellent Research Team of Lanzhou Jiaotong University, China (Grant No. 201803).

†Corresponding author. E-mail: weixp2008@gmail.com

© 2020 Chinese Physical Society and IOP Publishing Ltd

alloys.[49–51] Therefore, it is worth to explore whether the quaternary Heusler alloys with Cr, Zr, and Co elements still have the half-metallicity and high Curie temperature or other fancy properties. In this paper, we systematically study the structural, electronic, and magnetic properties together with exchange interactions and Curie temperatures of CrZrCoZ (Z = Al, Ga, In, Tl, Si, Pb) quaternary Heusler alloys.

2. Calculation details

In the present calculations, the full-potential local-orbital minimum-basis band-structure method (FPLO) is used to calculate the structural, electronic, and magnetic properties.[52,53] In this scheme, the scalar relativistic Dirac equation is solved, and the number of k-points in the Brillouin zone is set to $20 \times 20 \times 20$ in order to ensure the convergence of the calculated parameters. The convergence of the total energy is set to be better than 10^{-8} Hartree together with that of the density better than 10^{-6} in internal unit of the code, more details can be found in Ref. [50]. Heisenberg exchange coupling parameters can be obtained by the spin-polarized relativistic Korringa–Kohn–Rostoker package Munich SPRKKR.[54] An angular momentum cutoff of $\ell_{\max} = 3$ and $22 \times 22 \times 22$ k-points in each Brillouin zone direction are used in the calculations. In order to further improve the charge convergence with respect to $l_{\max}$, the Lloyd's formula is used to determine the Fermi level,[55,56] the details of calculations can be found from our previous works.[61,62] The elastic constants are calculated by using the Vienna *ab initio* simulation package (VASP).[57,58] The projected augmented wave (PAW) potentials and the Broyden–Fletcher–Goldfarb–Shanno (BFGS) algorithm are applied to fully relax all atomic positions, cell shapes, and cell volumes to achieve the minimum total energies of the systems. The cutoff energy for the plane wave expansion is 600 eV for all models, and the k-mesh is chosen as $20 \times 20 \times 20$ in each Brillouin zone. The total energy and force convergences are 10^{-5} eV per atom and 0.01 eV·Å^{-1}, respectively. In addition, the Perdew–Burke–Ernzerhof in the frame of generalized gradient approximation is used to describe the exchange–correlation potential in all calculations.[59]

3. Results and discussion

3.1. Structural properties

Quaternary Heusler alloys CrZrCoZ (Z = Al, Ga, In, Tl, Si, Pb) usually crystallize with three possible structures as shown in Table 1.

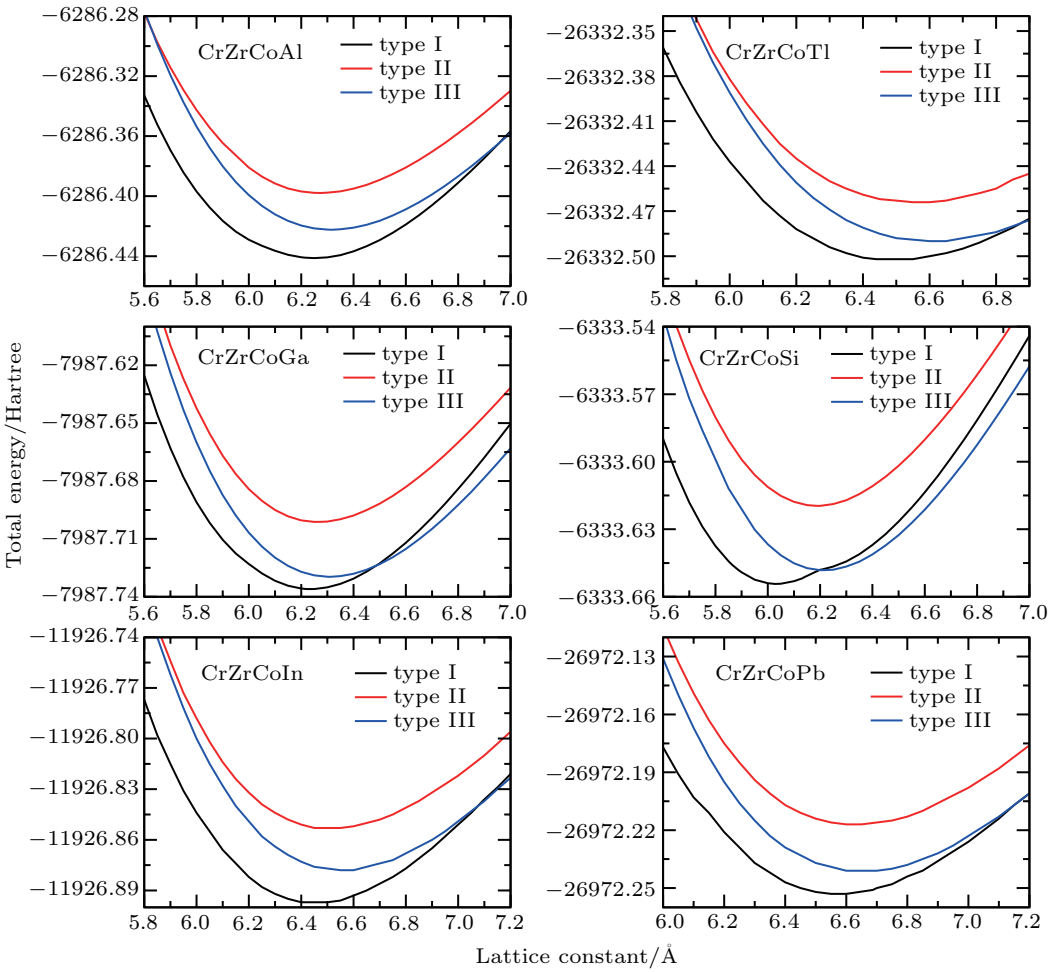


Fig. 1. Changes of total energies as a function of lattice constants for three possible structures of CrZrCoZ alloys.

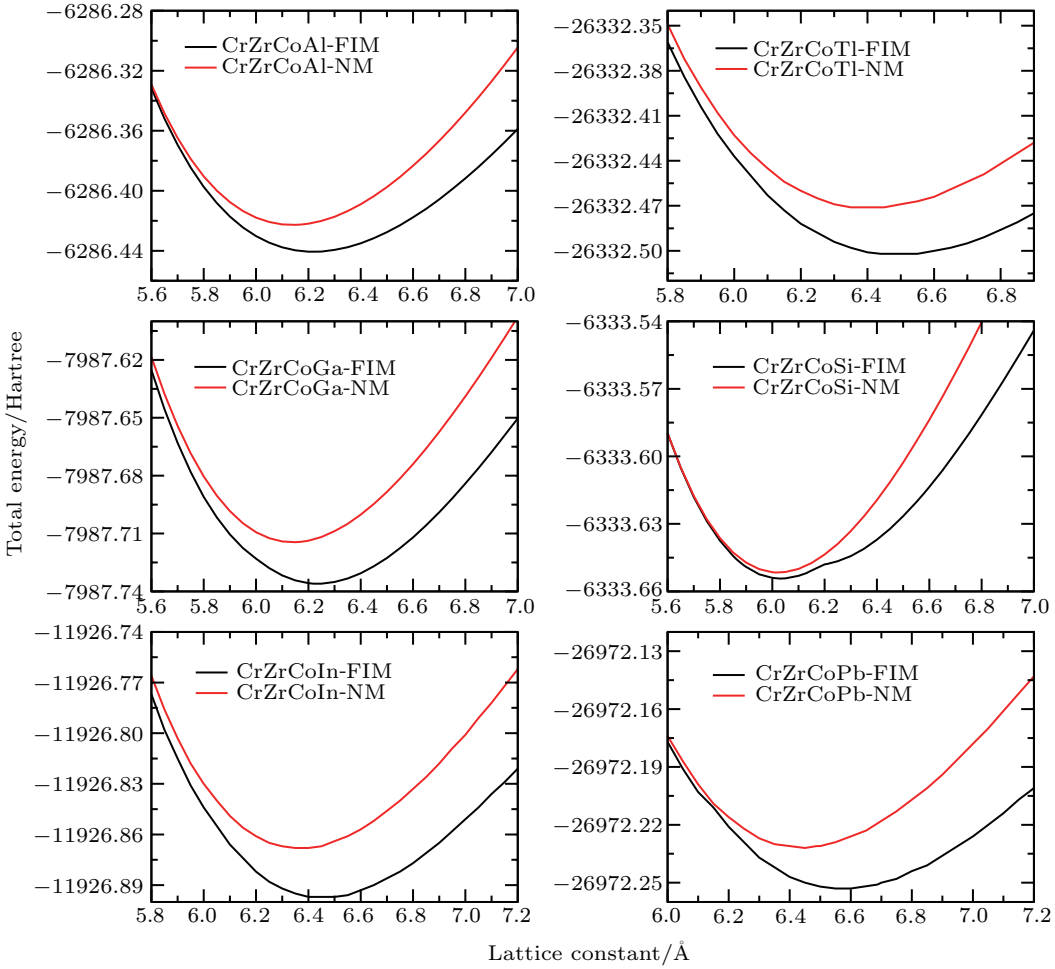


Fig. 2. Total energies of nonmagnetic and ferrimagnetic phases as a function of lattice constants for CrZrCoZ alloys.

Table 1. Three possible structures for quaternary Heusler alloys $XX'YZ$ (CrZrCoZ).

Structure	A(0,0,0)	B($\frac{1}{4},\frac{1}{4},\frac{1}{4}$)	C($\frac{1}{2},\frac{1}{2},\frac{1}{2}$)	D($\frac{3}{4},\frac{3}{4},\frac{3}{4}$)
Type I	X	X'	Y	Z
Type II	X'	X	Y	Z
Type III	X	Y	X'	Z

Therefore, we compare the total energies of the three possible structures in Fig. 1 to obtain the stable structure. It is found that the type I structure is the most stable. For the type I structure, we make a comparison of the total energies between nonmagnetic (NM) and ferrimagnetic (FIM) phases in Fig. 2, and find that the ferrimagnetic ground states have lower total energies. Accordingly, we tabulate the calculated lattice parameters in Table 2. Furthermore, we check the magnetic stability of the CrZrCoZ alloys by using Stoner model. In the simplified version of this theory, the Stoner criterion for spin polarization is $IN_0 > 1$, where I is the exchange integral (Stoner parameter) and N_0 is the density of states (DOS) of the ground state at the Fermi level. The exchange integral is determined by using the following formula:

$$\chi = \frac{N_0}{1 - IN_0}, \tag{1}$$

where the susceptibility is calculated by

$$\frac{1}{\chi} = \frac{\partial^2 E(m)}{\partial m^2}. \tag{2}$$

The $E(m)$ curves in Eq. (2) are calculated by the fixed spin moment method. The DOS N_0 at the Fermi level and the exchange integral I are estimated from Eq. (1), and their products (IN_0) are listed in Table 2. As is shown, the products IN_0 of the CrZrCoZ alloys are larger than 1, indicating that these alloys have magnetic ground states, it is also well consistent with our obtained total energy curves in Fig. 2. In addition, because the exchange splitting is proportional to Im^2, thus the larger exchange constants can generally lead to higher Curie temperature according to the mean field consideration.[60] Based on the calculated exchange integral and total magnetic moments, it is believed that the CrZrCoPb alloy has the highest Curie temperature among the CrZrCoZ alloys. In the following, we discuss the structural stability of CrZrCoZ alloys from the point views of thermodynamics and mechanical properties.

Firstly, the thermodynamic stability is measured by the formation energy E_f,

$$E_f = E_{tot} - \sum_i \mu_i x_i, \tag{3}$$

where E_{tot} is the calculated total energy per formula unit of the ground state, μ_i is the chemical potential of element i, and x_i

Table 2. Lattice constant at equilibrium (a_{cal}), density of states (N_0) at the Fermi level in nonmagnetic states, and the exchange integral (I) of CrZrCoZ alloys and its products with N_0 (IN_0). The spin-flip gap (E_{sfg}), band gap (E_g), and formation energy (E_f) per atom as well as Curie temperatures (T_C) are also shown.

Compounds	a_{cal}/Å	I/eV	N_0/eV^{-1}	IN_0	E_{sfg}/eV	E_g/eV	E_f/eV	T_C/K
CrZrCoAl	6.216	0.450	4.345	1.957	0.002	0.941	–0.186	975.78
CrZrCoGa	6.220	0.525	4.011	2.107	0.054	0.899	–0.143	1024.70
CrZrCoIn	6.422	0.668	3.598	2.403	0.225	0.843	–0.036	1046.40
CrZrCoTl	6.440	0.690	3.671	2.533	0.259	0.782	0.208	1034.21
CrZrCoSi	6.028	0.247	11.856	2.940	0.123	0.269	–0.191	68.42
CrZrCoPb	6.687	1.455	1.679	2.445	0.062	0.589	0.234	1482.60

is the quantity of element i in the alloys. From the E_f summarized in Table 2, we can see that the CrZrCoZ (Z = Al, Ga, In, Si) alloys have negative formation energies, indicating that they can be easily fabricated in experiment. However, the positive formation energies for CrZrCoTl and CrZrCoPb alloys imply that they are thermodynamically unstable, but they may can be synthesized in the Heusler phase in a non-equilibrium process.[63]

The mechanical properties of material are crucial in engineering technological applications. Therefore, we calculate the elastic constants of the CrZrCoZ alloys, which not only offer related mechanical parameters, but also can be used to check their mechanical stability by using the Born–Huang criteria as follows:

$$B = \frac{C_{11}+2C_{12}}{3} > 0,$$
$$C_{11}-C_{12} > 0, \quad C_{44} > 0. \tag{4}$$

We can find from Table 3 that the CrZrCoZ (Z = Al, Ga, In, Tl, Si) alloys satisfy the stability conditions. Furthermore, these elastic constants are applied to evaluate the elastic moduli, including bulk modulus B, shear modulus G, etc. in the following relations:

$$B = \frac{C_{11}+2C_{12}}{3}, \tag{5}$$
$$G_R = \frac{5C_{44}(C_{11}-C_{12})}{4C_{44}+(C_{11}-C_{12})}, \tag{6}$$
$$G_V = \frac{C_{11}-C_{12}+3C_{44}}{5}, \tag{7}$$

where G_R and G_V are the Reuss's and Voigt's shear moduli, and their arithmetic average is estimated by using the Voigt–Reuss–Hill approximation in the following equation:

$$G = \frac{G_V+G_R}{2}. \tag{8}$$

In addition, Young's modulus E, Poisson's ratio υ, and anisotropy factor A are obtained as follows:

$$E = \frac{9BG}{3B+G}, \tag{9}$$
$$\upsilon = \frac{3B-2G}{2(3B+G)}, \tag{10}$$
$$A = \frac{2C_{44}}{C_{11}-C_{12}}. \tag{11}$$

In Table 3, we list these moduli parameters. Among them, the bulk modulus B is used to measure the material's resistance against compression, whereas Young's modulus E provides the information about stiffness where the higher value corresponds to a stiffer material. The results show that the B, E, and G values of CrZrCoSi are highest among the alloys. The ratio of the transverse contraction to the longitudinal extension in the direction of elastic loading is defined as Poisson's ratio υ, where the lower limit of υ for most metals is about 0.25. Apart from the CrZrCoPb alloy, the calculated υ values range from 0.329 to 0.366. In addition, it should be mentioned that the B, E, G, and υ values of CrZrCoSi are higher than those of Zr_2CoSi, and its A is lower than that of Zr_2CoSi.[64] The calculated anisotropy factor A deviates from unity, indicating an anisotropic elastic behavior. According to the Pugh's criteria, the CrZrCoZ alloys show a ductile behavior. Furthermore, the melting temperature is obtained in the following empirical relation:[65]

$$T_{melt} = 607 + 9.3 \times B \pm 555. \tag{12}$$

It is found that the melting temperature of CrZrCoSi is highest due to its highest bulk modulus (see Table 3).

Table 3. The calculated elastic constants C_{ij} (in GPa), bulk modulus B (in GPa), Young's modulus E (in GPa), isotropic shear modulus G (in GPa), Poisson's ratios υ, anisotropy factor A, Pugh's ratio B/G, and the melting temperature T_{melt} (in K) of CrZrCoZ (Z = Al, Ga, In, Tl, Si, Pb) alloys.

Alloys	C_{11}	C_{12}	C_{44}	B	G_V	G_R	G	E	υ	A	B/G	T_{melt}
CrZrCoAl	172.74	112.81	73.05	132.78	55.82	46.37	51.09	135.87	0.329	2.438	2.598	1841.93
CrZrCoGa	163.89	124.87	68.09	137.88	48.66	34.11	41.38	112.86	0.363	3.490	3.331	1889.28
CrZrCoIn	159.92	109.41	68.39	126.25	51.13	40.63	45.88	122.78	0.337	2.707	2.751	1781.15
CrZrCoTl	141.59	108.73	58.58	119.68	41.72	28.91	35.31	96.46	0.365	3.564	3.388	1720.08
CrZrCoSi	252.14	138.47	48.27	176.36	51.70	51.37	51.53	140.88	0.366	0.849	3.422	2247.18
CrZrCoPb	–25.45	–31.48	34.67	–29.47	22.01	6.66	14.33	51.35	0.790	11.503	–2.055	332.88

3.2. Electronic structures

In Fig. 3, we give the total density of states (DOS) and partial density of states (PDOS) of CrZrCoZ (Z = Al, Ga, In, Tl, Si, Pb) alloys at their respective equilibrium states. It is evident that the CrZrCoZ alloys preserve a half-metallic behavior. An energy gap appears at the Fermi level in the minority-spin channel for the CrZrCoZ (Z = Al, Ga, In, Tl, Pb) alloys, while there is nonzero DOS in the majority-spin channel. By contrast, for the CrZrCoSi alloy, the gap is pinned in the majority-spin channel, and the states exist in the minority-spin channel. The striking difference is ascribed to its smallest exchange integral (see Table 2), which leads to the incomplete exchange splitting between e_g and t_{2g} states (see Fig. 5), and then the gap of CrZrCoSi is pinned in the majority-spin channel. In fact, a bigger exchange integral can make the exchange splitting stronger, and the gap larger. Particularly, for the CrZrCoSi alloy, the Cr-3d states offer a major contribution to the total DOS in the energy range between −1 eV and 0.5 eV in both spin channels. While for the CrZrCoZ (Z = Al, Ga, In, Tl, Pb) alloys, the strong hybridizations between Zr-4d and Co-3d states lead to an energy distribution spreading from 0 eV to 1 eV in the spin-down states, and they almost have the same contribution to the total DOS in the minority-spin states above the Fermi level, it is mainly governed by the Co-3d states from −3 eV to 0 eV below the Fermi level, and the spin-up states are briefly occupied by Co-3d and Cr-3d states. More evidently, there is a saddle point from Γ to X direction in the majority-spin of energy dispersion pictures for CrZrCoZ (Z = Al, Ga, In, Tl) alloys (see Fig. 4), indicating high DOS values. Overall, in the CrZrCoZ alloys, the obvious hybridizations between d–d states lead to the formation of the gap.

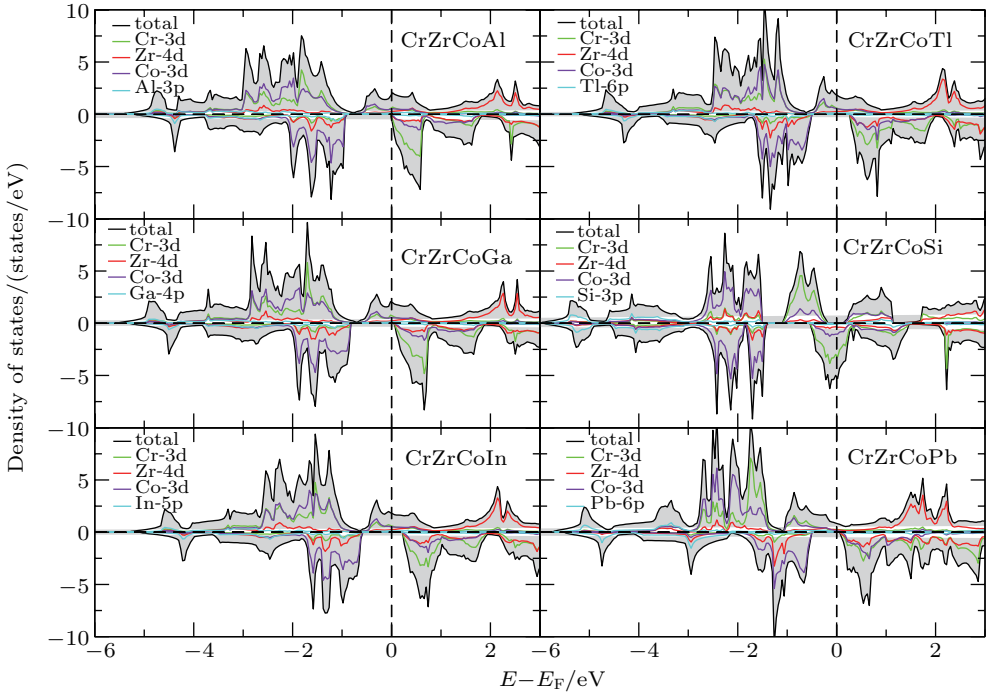


Fig. 3. Total and paritial density of states for CrZrCoZ alloys.

In order to understand the electronic properties in depth, we analyze the local density of states (LDOS) in Fig. 5. It is clear that these alloys can be in quality classified into two types according to their gaps in the spin channels. For the CrZrCoZ (Z = Al, Ga, In, Tl, Pb) alloys, taking the CrZrCoAl as an example, we can notice that the d states are divided into t_{2g} and e_g states for Cr, Zr, and Co atoms in the octahedral crystal field, the difference between e_g and t_{2g} states for Cr and Co atoms is bigger than that of Zr atom. Thus, we conclude that the exchange splitting between e_g and t_{2g} states from Cr and Co atoms leads mainly to the formation of the spin-flip gap. In detail, both t_{2g} and e_g are unoccupied in the spin down channel for the Cr atom. In the spin up channel, the t_{2g} states are fully occupied, leading to 3 μ_B contribution to the magnetic moment. As to the e_g state, it is partially occupied, making 0.5 μ_B contribution. Thus, the magnetic moment of the Cr atom is about 3.5 μ_B. On the other hand, the Co magnetic moment, which arises from the complex crystal splitting, is 0.88 μ_B, the hybridization between Co and Cr atoms is so strong that we can not use an atomic model to analysis it. While for the CrZrCoSi alloy, the same situation is observed. Also, it is found that the t_{2g} and e_g states almost have equivalent splitting strengths for the Co atom. In addition, we can see from the band pictures in Fig. 4 that the indirect band gap from K to L direction is observed in CrZrCoZ (Z = Ga, In, Tl, Pb) alloys, and it is a direct band gap for CrZrCoAl and CrZrCoSi alloys

from K to Γ direction and Γ point, respectively. Accordingly, the spin-flip gap, which is defined as the minimum energy required to flip the minority-spin electrons of conduction band minimum (CBM) to valence band for CrZrCoZ (Z = Al, Ga, In, Tl, Pb) alloys, and it is the minimum energy required to flip the majority-spin electrons of valence band maximum (VBM) to conduction band for CrZrCoSi, is labeled in the bands. In Table 2, we tabulate the band gap and the spin-flip gap, and observe that the CrZrCoSi alloy has the lowest band gap up to 0.269 eV because of its smallest exchange integral, and the spin-flip gap is the biggest for the CrZrCoPb alloy.

The half-metallic properties usually can be affected by lattice constants. Moreover, the half-metal is often used in the form of thin films in spintronic devices, where the lattice parameters are strongly determined by the growth substrate. Therefore, it is necessary to study the robustness of the half-metallicity on the lattice constants. In Fig. 6, we offer the CBM and VBM in the spin down channel as a function of the lattice constants for CrZrCoZ (Z = Al, Ga, In, Tl, Pb) alloys. By contrast, they are from the spin-up channel for the CrZrCoSi alloy. It can be seen from Fig. 6 that the half-metallicity can be preserved within the range of 6.212–7.053 Å, 6.169–6.997 Å, 6.189–7.055 Å, 6.163–7.009 Å, and 6.651–6.883 Å for CrZrCoAl, CrZrCoGa, CrZrCoIn, CrZrCoTl, and CrZrCoPb alloys, respectively. While for the CrZrCoSi alloy, the half-metallicity is kept in the lattice constants of 5.864–6.149 Å and 6.577–6.878 Å, where the disappearance of half-metallicity between 6.149 Å and 6.577 Å may ascribe to the occurrence of phase transition. For the CrZrCoZ (Z = Al, Ga, In, Tl) alloys, when the lattice constants are larger than 7.053 Å, 6.997 Å, 7.055 Å, and 7.009 Å, the Fermi level has an intersection with the valence bands, which leads to the loss of the half-metallicity although the band gap is still kept in the spin down channel. It is the intersection of the Fermi level and the conduction bands when the lattice constants are compressed to 6.212 Å, 6.169 Å, 6.189 Å, and 6.163 Å, also leading to the loss of the half-metallicity, which is different from the cases of the lattice expansion. Thus, we can say that the CrZrCoZ (Z = Al, Ga, In, Tl) alloys have a good robustness of half-metallic properties against the lattice change and are possible ideal candidates for applying in a quite wider temperature range.

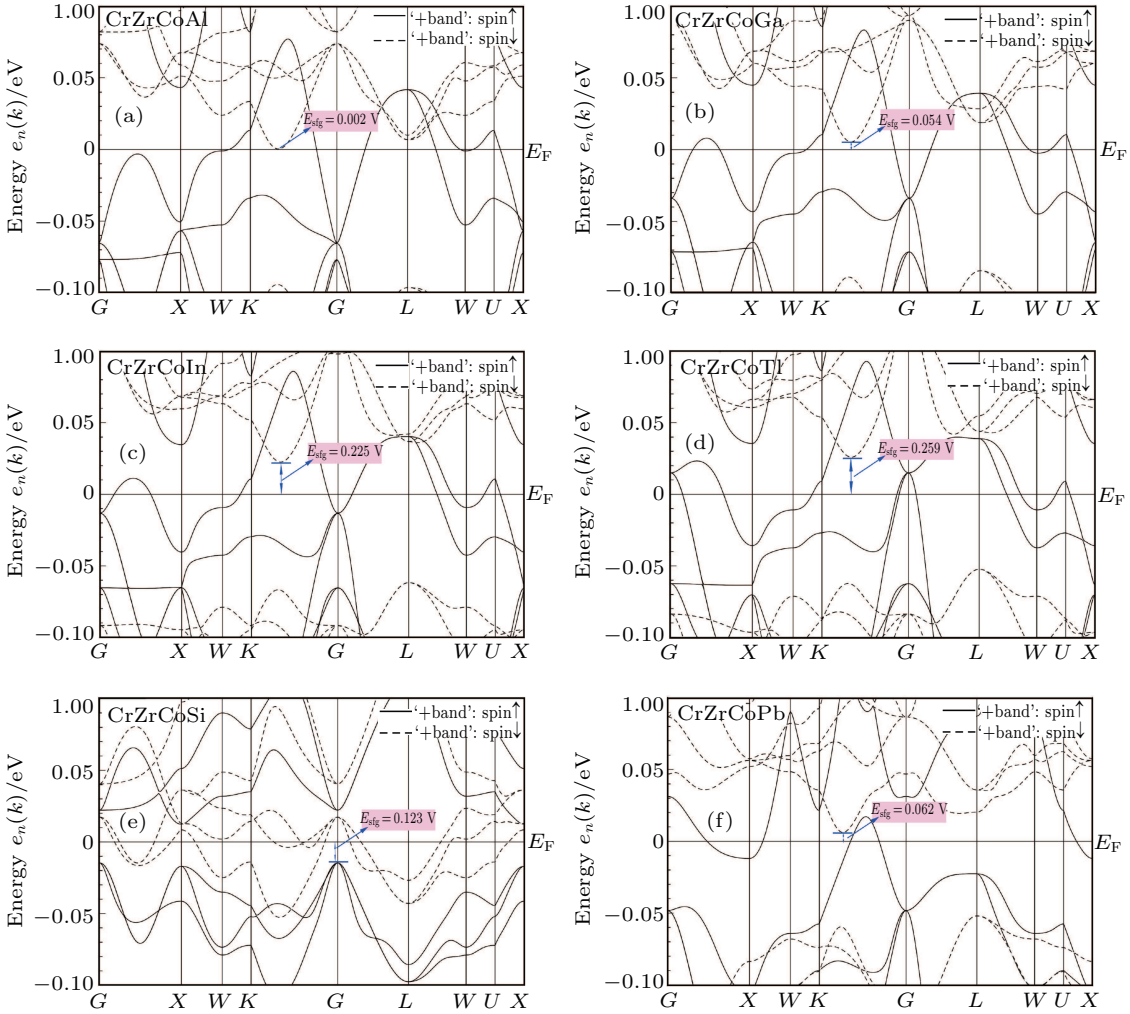


Fig. 4. Band structures for CrZrCoZ alloys. Note that the spin-flip gap is labeled.

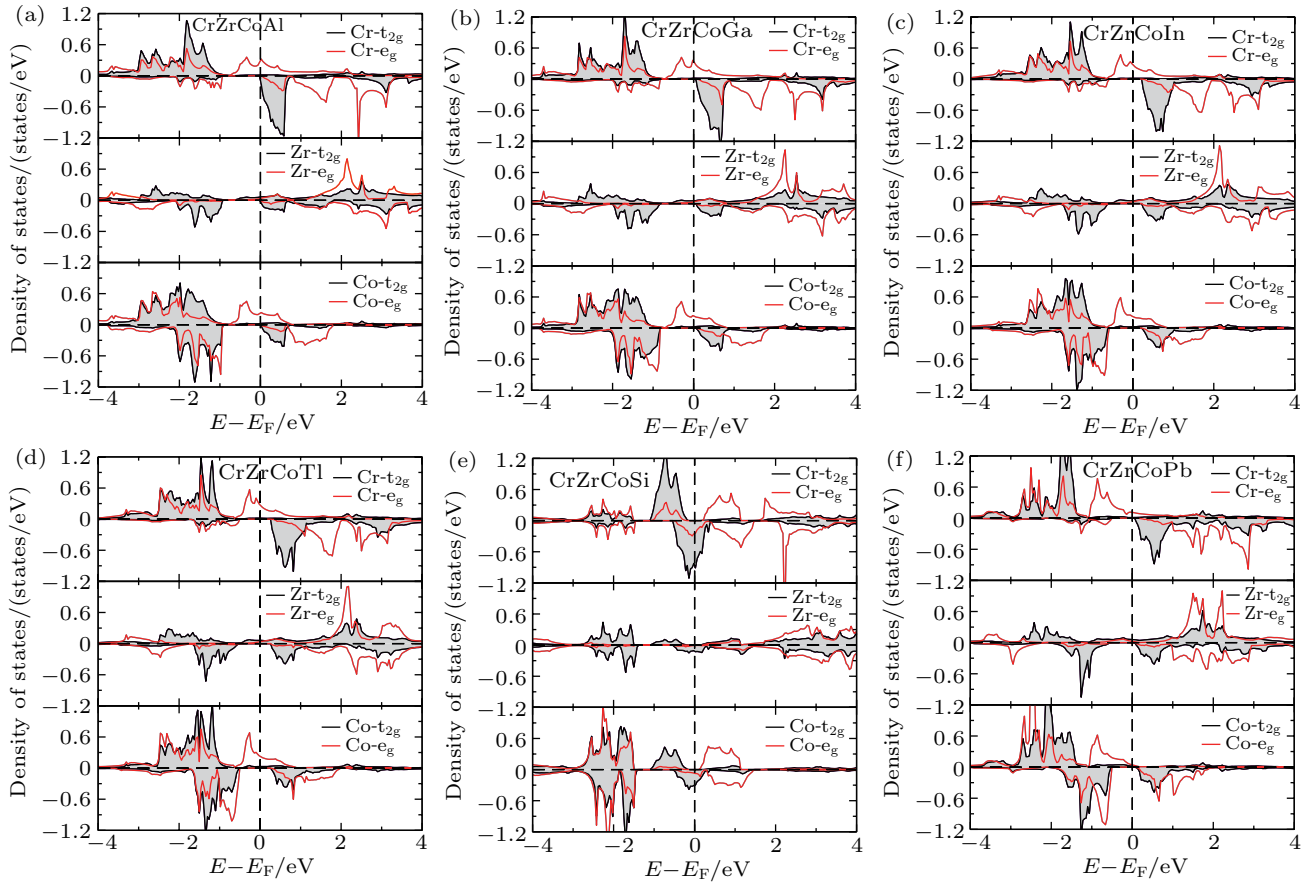


Fig. 5. Local density of states of CrZrCoZ alloys.

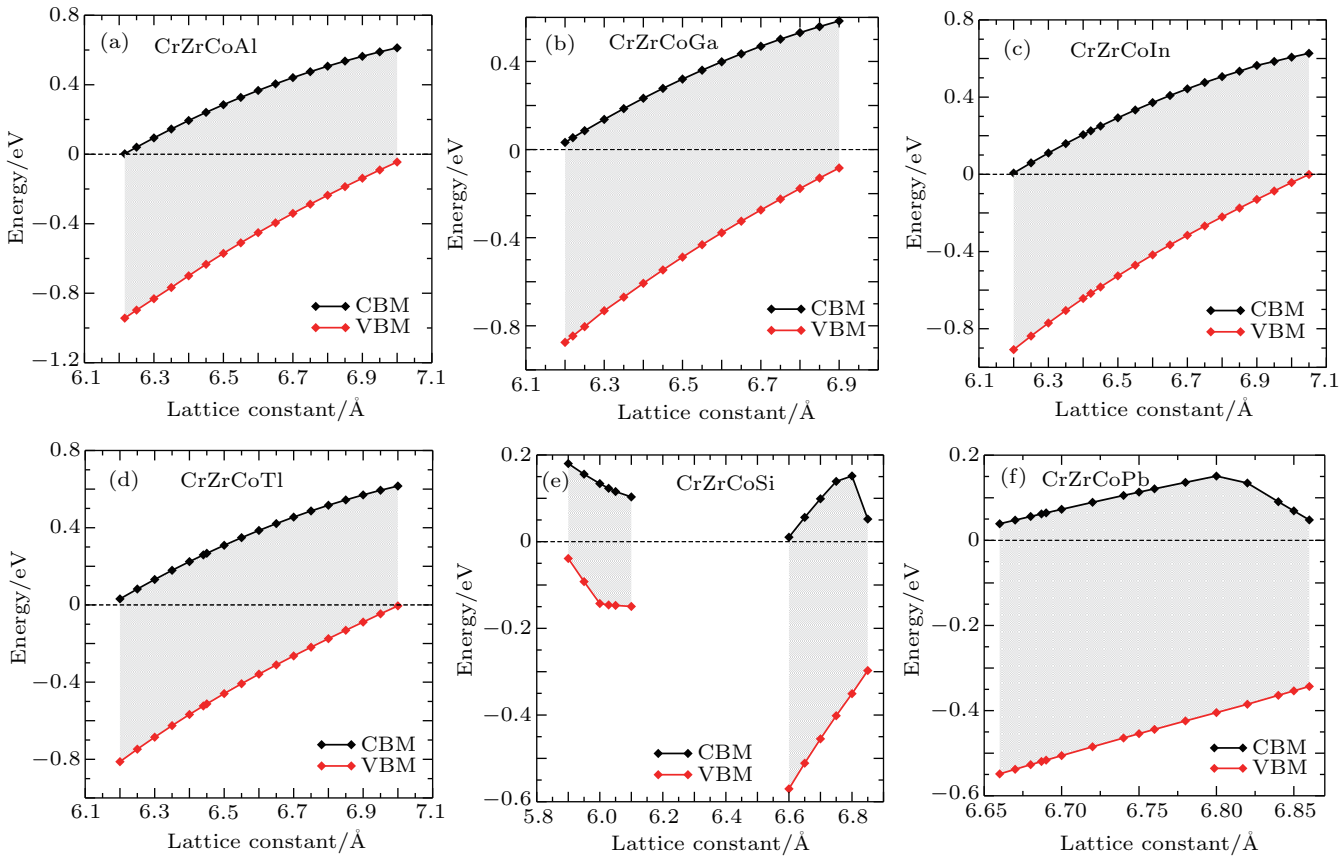


Fig. 6. Changes of VBM and CBM for CrZrCoZ alloys depend on the lattice constants.

3.3. Magnetic properties

In this section, we focus on the magnetic moments of CrZrCoZ alloys, as expected, the calculated total magnetic moments are an integer because of their itinerant valence electrons, which is also a unique property for half-metal, and the calculated total magnetic moments obey the Slater–Pauling rule.[67,68] Besides, we also notice that the total magnetic moments for all alloys are mainly carried by the Cr atoms, and the other atoms offer rather small contribution. In addition, the magnetic moments of the Zr and Z atoms are anti-parallel with the Cr and Co magnetic moments, thus the CrZrCoZ alloys are ferrimagnetic half-metals. For the CrZrCoZ (Z = Al, Ga, In, Tl, Pb) alloys, their integral magnetic moments can be illustrated by the occupied electronic states in Fig. 7(a), i.e, the Cr and Co atoms located at A and C sites have the octahedral symmetry (see Fig. 7(b)), and their d-orbitals hybridize with each other, then creating five bonding triple-degenerated t_{2g} and double-degenerated e_g states, and five anti-bonding triple-degenerated t_{1u} and double-degenerated e_u states, and the energies of the t_{2g} and e_u states are higher than those of e_g and t_{1u}. In turn, the five bonding d-hybrids hybridize with the Zr-d orbitals, creating again bonding and anti-bonding states. In addition, the Z element provides a single s state and triple-degenerated p states, and partially accommodate d-charge from the Cr, Zr, and Co atoms, therefore, there are nine occupied electronic states in total, thus their total magnetic moments follow the Slater–Pauling rule $M_t = Z_t - 18$, where M_t is the total magnetic moment, and Z_t is the total valence number per formula unit. While for the CrZrCoSi alloy, the occupation of electronic states is the same as that of the CrZrCoZ (Z = Al, Ga, In, Tl, Pb) alloys, the triple-degenerated t_{1u} states are only localized in the occupied states due to lower exchange splitting energy, then leading to twelve occupied electronic states, thus its total magnetic moment obeys the Slater–Pauling rule $M_t = 24 - Z_t$ (see Fig. 7(c)).

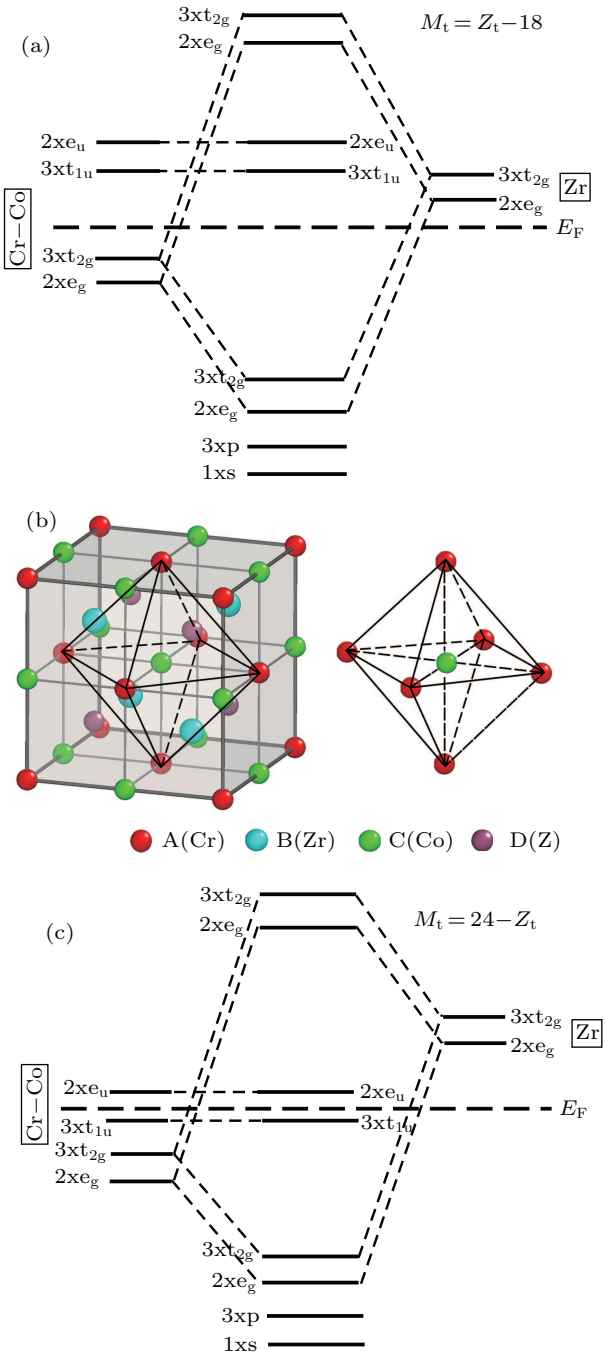


Fig. 7. Orbital hybridizations under the crystal field for (a) CrZrCoZ (Z = Al, Ga, In, Tl, Ge, Pb) alloys, (c) CrZrCoSi alloy, and (b) crystal structure and field symmetry in CrZrCoZ alloys.

Table 4. Total and atomic magnetic moments (in μ_B) for CrZrCoZ (Z = Al, Ga, In, Tl, Si, Pb) alloys.

Alloys	M_t	Cr	Zr	Co	Z
CrZrCoAl	4.000	3.528	–0.237	0.888	–0.179
CrZrCoGa	4.000	3.570	–0.256	0.832	–0.146
CrZrCoIn	4.000	3.711	–0.331	0.786	–0.166
CrZrCoTl	4.000	3.746	–0.341	0.752	–0.157
CrZrCoSi	1.000	1.068	–0.009	0.015	–0.074
CrZrCoPb	5.000	4.061	–0.335	1.382	–0.108

3.4. Exchange interactions and Curie temperatures

In Fig. 8, we show the calculated Heisenberg exchange coupling parameters J_{ij}.[66] It is notable that J_{ij} of the CrZrCoZ alloys is tightly confined to clusters of radius $r \leq 2.0a$, and the Co(C)–Cr(A) exchange values decrease slightly as the atomic radius and electronegativity increase when Z is of III group. In particular, for the CrZrCoAl alloy, the first, second, and third nearest neighbors of Co(C)–Cr(A) interactions show positive coupling values, implying ferromagnetic exchanges. While for the Cr(A)–Cr(A) exchange, the first and third nearest neighbors are positive values, it is negative for the second nearest neighbor, indicating their anti-parallel coupling. For the CrZrCoGa, CrZrCoIn, and CrZrCoTl alloys, these exchanges are the same as those in the CrZrCoAl alloy, thus leaving them no discussion. For the CrZrCoSi alloy, the Co(C)–Cr(A) and Co(C)–Co(C) exchanges indicate the obvious oscillation behavior, and the three nearest neighbors for

Cr(A)–Cr(A) exchange show negative values, implying antiferromagnetic interactions. In the CrZrCoPb alloy, the Co(A)–Cr(A) exchange plays a leading role in interactions, its first, second, and third interactions are positive, and notably higher than those in CrZrCoSi because of the larger local magnetic moments. The other exchanges are not shown in Fig. 8 due to their smaller interactions. Accordingly, the oscillatory behavior in all interactions indicates a RKKY exchange.[69] In fact, a positive J_{ij} can improve the Curie temperature, and a negative J_{ij} can reduce the Curie temperature. Furthermore, we offer the sum J_0 of exchange coupling parameters J_{ij}, these values are given in Table 5. It can be seen that the Cr(A)–Cr(A) and Cr(A)–Zr(B) exchanges lead to the appearance of ferrimagnetic states in CrZrCoZ (Z = Al, Ga, In, Tl, Pb) alloys. By comparison, the Cr(A)–Zr(B) and Zr(B)–Zr(B) exchanges play a leading role in CrZrCoSi alloy. According to the calculated J_0, we construct a 4×4 J_0 matrix to obtain the Curie temperature (see Table 2), the details of calculations can be found from Ref. [19]. It finds that the CrZrCoZ (Z = Al, Ga, In, Tl, Pb) alloys have noticeably higher Curie temperatures than room temperature, and the tendency of the Curie temperatures is well consistent with the Im^2.

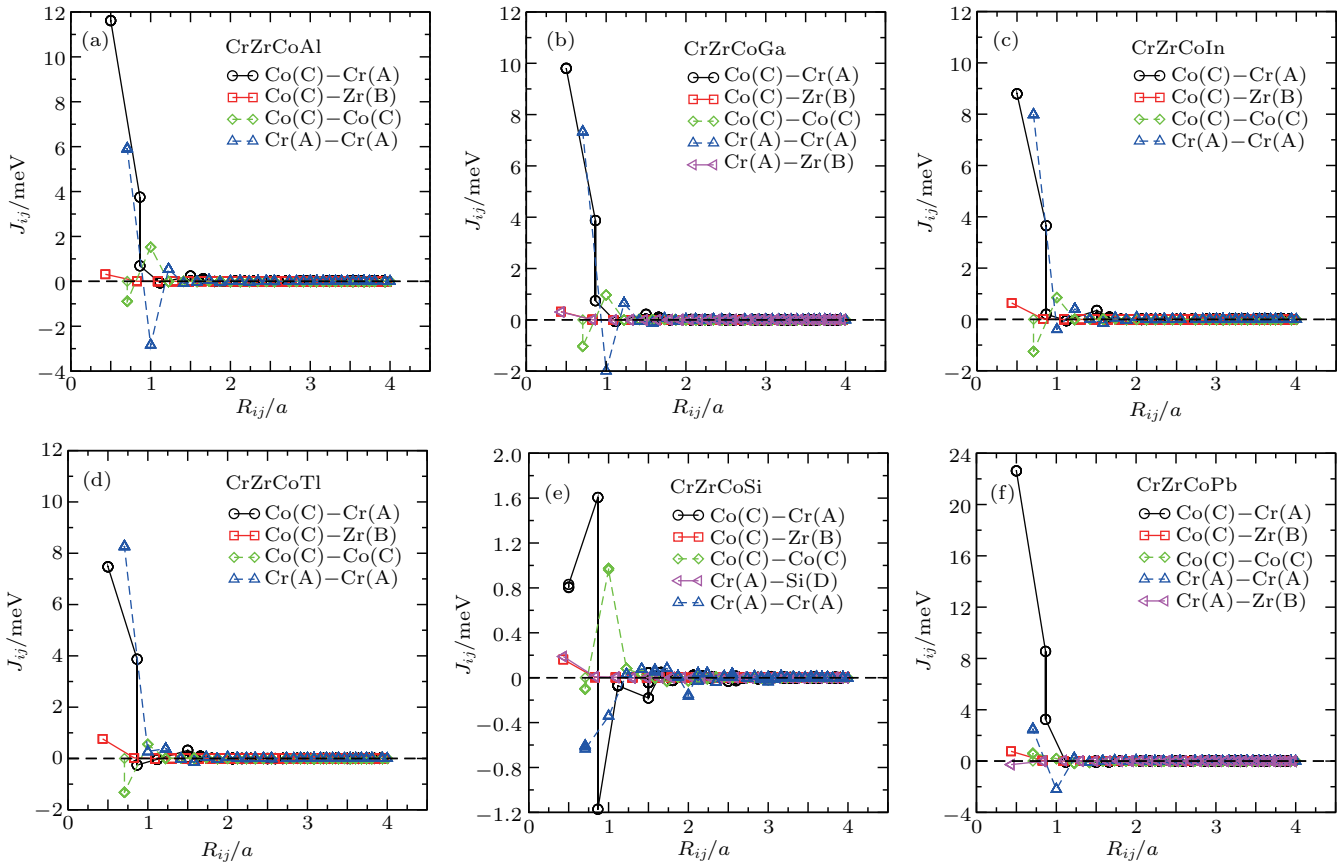


Fig. 8. Exchange interactions J_{ij} for CrZrCoZ alloys with the interatomic distance r.

Table 5. Exchange coupling parameters J_0 (in meV) between the constituents are tabulated. Note that the subscripts 1, 2, 3, and 4 correspond to the Cr, Co, Zr, and Z atoms, respectively.

Alloys	J_{11}	J_{12}	J_{13}	J_{14}	J_{22}	J_{23}	J_{24}	J_{33}	J_{34}	J_{44}
CrZrCoAl	63.239	0.766	89.781	–0.151	–0.009	1.318	–0.028	–1.723	0.597	–0.006
CrZrCoGa	87.125	1.213	79.441	0.267	–0.009	1.342	–0.036	–6.343	0.571	–0.008
CrZrCoIn	100.118	0.206	71.401	0.054	–0.037	2.740	–0.032	–9.233	0.459	–0.003
CrZrCoTl	106.908	0.145	62.537	0.051	–0.050	3.289	–0.024	–11.673	0.311	–0.001
CrZrCoSi	–4.907	–0.052	3.790	0.889	–0.002	0.747	–0.024	7.728	0.167	–0.006
CrZrCoPb	21.656	–0.829	178.941	–0.017	–0.076	3.769	–0.016	3.611	0.093	0.000

4. Summary and conclusions

The first-principle calculations are used to study the structural, electronic, magnetic properties along with exchange interactions and Curie temperatures of quaternary Heusler alloys CrZrCoZ (Z = Al, Ga, In, Tl, Si, Pb). The results show that the CrZrCoZ alloys are ferrimagnetic half-metals, and their integral magnetic moments obey the Salter–Pauling rule. Stability analysis indicates that the CrZrCoZ alloys have magnetic ground states, and the CrZrCoAl, CrZrCoGa, CrZrCoIn, and CrZrCoSi alloys are likely to be prepared in experiment.

Occupation of electronic states shows that there are nine occupied states for CrZrCoZ (Z = Al, Ga, In, Tl, Pb) alloys, thus their total magnetic moments obey the Salter–Pauling rule $M_t = Z_t - 18$. For the CrZrCoSi alloy, the total magnetic moment follows the Sater–Pauling rule $M_t = 24 - Z_t$ due to its twelve occupied states, the exchange splitting between e_g and t_{2g} states from the Cr and Co atoms leads mainly to the formation of spin-flip gap. In addition, a good half-metallic robustness against the lattice changes is also observed in CrZrCoZ (Z = Al, Ga, In, Tl) alloys. According to the calculated Heisenberg exchange coupling parameters, we find that the Cr(A)–Cr(A) and Cr(A)–Zr(B) exchanges lead to the formation of ferrimagnetic states of CrZrCoZ (Z = Al, Ga, In, Tl, Pb) alloys, and it is the Cr(A)–Zr(B) and Zr(B)–Zr(B) exchanges for CrZrCoSi alloy. Finally, we estimate the Curie temperatures of CrZrCoZ by using mean-field approximation, the Curie temperatures of CrZrCoZ (Z = Al, Ga, In, Tl, Pb) alloys are noticeably higher than room temperature. Thus, our results may offer a valuable hint for CrZrCoZ alloys in future spintronic applications.

References

[1] Jourdan M, Minar J, Braun J, *et al.* 2014 *Nat. Commun.* **5** 3974
[2] Li G N and Jin Y J 2009 *Chin. Phys. Lett.* **26** 107101
[3] Zhao K, Zhang K, Wang J J, Yu J and Wu S X 2011 *Acta Phys. Sin.* **60** 127101 (in Chinese)
[4] Cheng Z M, Wang X Q, Wang F, Lu L Y, Liu G B, Duan Z F and NieZ X 2011 *Acta Phys. Sin.* **60** 096301 (in Chinese)
[5] Gao Y C, Wang X T and Habib R 2015 *Chin. Phys. B* **24** 67102
[6] Liu Z H, Zhang M, Cui Y T, Zhou Y Q, Wang W H and Wu G H 2003 *Appl. Phys. Lett.* **82** 424
[7] Kainuma R, lmano Y, lto W, Morito H, Sutou Y, Oikawa K, Fujita Aand lshaida K 2006 *Appl. Phys. Lett.* **88** 192513
[8] Tan C L, Tian X H and Cai W 2008 *Chin. Phys. Lett.* **25** 3372
[9] Chen J, Li Y, Shang J X and Xu H B 2009 *Chin. Phys. Lett.* **26** 47101
[10] Zhao J J, Shu D, Qi X, Liu E K, Zhu W, Feng L, Wang W H and Wu G H 2011 *Acta Phys. Sin.* **60** 107203 (in Chinese)
[11] Li G T, Liu Z H, Meng F Y, Ma X Q and Wu G H 2013 *Chin. Phys. B* **22** 126201
[12] Bainsla L, Mallick A I, Raja M M, Nigam A K, Varaprasad B S D ChS, Takahashi Y K, Alam A, Suresh K G and Hono K 2015 *Phys. Rev. B* **91** 104408
[13] Xu G Z, Liu E K, Du Y, Li G J, Liu G D, Wang W H and Wu G H 2013 *Europhys. Lett.* **102** 17007
[14] Gao Q, Xie H H, Li L, Lei G, Wang K, Deng J B and Hu X R 2015 *Superlattice Microst.* **85** 536
[15] Gao Q, Opahle I and Zhang H B 2019 *Phys. Rev. Materials* **3** 024410
[16] Khan M, Ali N and Stadler S 2007 *J. Phys. Appl.* **101** 053919
[17] Liu J, Gottschall T, Skokov K P, Moore J D and Gutfleisch O 2012 *Nat. Mater.* **11** 620
[18] Zhang X W 2018 *Chin. Phys. B* **27** 127101
[19] Wei X P, Gao P F and Zhang Y L 2020 *Curr. Appl. Phys.* **20** 593
[20] Wernick J H, Hull G W, Geballe T H, Bernardini J E and Waszczak J V 1983 *Mater. Lett.* **2** 90
[21] Wolf S A, Awschalom D D, Buhrman R A, Daughton J M, von MolnarS, Roukes M L, Chtchelkanova A Y and Treger D M 2001 *Science* **294** 1488
[22] Graf T, Felser C and Parkin S S P 2011 *Prog. Solid State Chem.* **39** 1
[23] Heusler F 1903 *Verh. DPG.* **5** 219
[24] Heusler F, Starck W and Haupt E 1903 *Verh. DPG.* **5** 220
[25] Drews J, Eberz U and Schuster H 1986 *J. Less-Common Met.* **116** 271
[26] Dai X, Liu G, Fecher G H, Felser C, Li Y and Liu H 2009 *J. Appl.Phys.* **105** 07E901
[27] Gao G Y, Hu L, Yao K L, Luo B and Liu N 2013 *J. Alloys Compd.* **551** 539
[28] Alijani V, Winterlik J, Feher G H, Naghavi S S and Felser C 2011 *Phys. Rev. B* **83** 184428
[29] Alijani V, Ouardi S, Fecher G H, Winterlik J, Naghavi S S, Kozina X, Stryganyuk G, Felser C, lkenaga E, Yamashita Y, Ueda S and Kobayashi K 2011 *Phys. Rev. B* **84** 224416
[30] Kundu A, Ghosh S, Banerjee R, Ghosh S and Sanyal B 2017 *Sci. Rep.* **7** 1803
[31] Kandpal H C, Ksenofontov V, Wojcik M, Seshadri R and Felser C 2007 *J. Phys. D: Appl. Phys.* **40** 1587
[32] Singh M, Saini H S, Thakur J, Reshak A H and Kashyap M K 2013 *J. Alloys Compd.* **580** 201
[33] Wang X T, Cui Y T, Liu X F and Liu G D 2015 *J. Magn. Mater. Magn.* **394** 50
[34] Gökoğlu G 2012 *Solid State Sci.* **14** 1273
[35] Rasool M N, Mehmood S, Sattar M A, Khan M A and Hussain A 2015 *J. Mag. Mag. Mater.* **395** 97
[36] Kubler J, Fecher G H and Felser C 2007 *Phys. Rev. B* **76** 024414
[37] Nehra J, Sudheesh V D, Lakshmi N, and Venugopalan K and 2013 *Phys. Status Solidi RRL* **7** 289
[38] Wang X T, Khachai H, Khenata R, *et al.* 2017 *Sci. Rep.* **7** 16183
[39] Feng L, Ma J, Yang Y, Lin T and Wang L 2018 *Appl. Sci.* **8** 2370
[40] Hoat D M 2019 *Chem. Phys.* **523** 130
[41] Enamullah Venkateswara Y, Gupta S, Varma M R, Singh P, Suresh K G and Alam A 2015 *Phys. Rev. B* **92** 224413
[42] Jain R, Jain V K, Chandra A R, Jain V and Lakshmi N 2018 *J. Supercond. Nov. Magn.* **31** 2399
[43] Bahnes A, Boukortt A, Abbassa H, Aimouch D E, Hayn R and Zaoui A 2018 *J. Alloys Compd.* **731** 1208
[44] Kang X H and Zhang J M 2017 *J. Phys. Chem. Solids* **105** 9
[45] Gao Y C and Gao X 2015 *AIP Adv.* **5** 057157
[46] Meinert M and Geisler M P 2013 *J. Magn. Mater. Magn.* **341** 72
[47] Mohanta S K, Tao Y X, Yan X Y, Qin G H, Chandragiri V, Li X, JingC, Cao S X, Zhang J C, Qiao Z H, Gu H and Ren W 2017 *J. Mater. Magn.* **430** 430
[48] Jin H S and Lee K W 2019 *Curr. Appl. Phys.* **19** 193
[49] Wei X P, Zhang Y L, Wang T, Sun X W, Song T, Guo P and Deng J B 2017 *Mater. Res. Bull.* **86** 139
[50] Wei X P, Gao P F, Zhang Y L and Zhang H B 2019 *J. Magn. Mater. Magn.* **477** 190
[51] Yan P L, Zhang J M and Xu K W 2015 *J. Magn. Mater. Magn.* **391** 43
[52] Koepernik K and Eschrig K 1999 *Phys. Rev. B* **59** 1743
[53] Opahle I, Koepernik K and Eschrig H 1999 *Phys. Rev. B* **60** 14035.
[54] Ebert H, Kodderitzsch D and Minar J 2011 *Rep. Prog. Phys.* **74** 096501
[55] Lloyd P and Smith P V 1972 *Adv. Phys.* **21** 69
[56] Zeller R 2008 *J. Phys.: Condens. Matter* **20** 035220
[57] Kresse G and Furthmuller J 1996 *Phys. Rev. B* **54** 11169
[58] Kresse G and Joubert D 1999 *Phys. Rev. B* **59** 1758
[59] Perdew J P, Burke K and Ernzerhof M 1996 *Phys. Rev. Lett.* **77** 3865
[60] Zhang W X, Song Z D, Peng B and Zhang W L 2012 *J. Appl. Phys.* **112** 043904
[61] Wei X P and Zhou Y H 2018 *Intermetallics* **93** 283
[62] Wei X P, Zhang Y L, Sun X W, Song T, Guo P, Gao Y, Zhang J L, ZhuX F and Deng J B 2017 *J. Alloys Compd.* **694** 1254
[63] Tanaka M A, Lshikawa Y, Wada Y, Hori S, Murata A, Horii S, Yamanishi Y, Mibu K, Kondou K, Ono T and Kasai S 2012 *J. Appl. Phys.* **111** 053902
[64] Yousuf S and Gupta D C 2017 *Mater. Res. Express* **4** 116307
[65] Johnston I D and Consortium for Upper Level Physics Software 1996 *Solid State Physics Simulations* (New York: Wiley)
[66] Liechtenstein A I, Katsnelson M I, Antropov V P and Gubanov V A 1987 *J. Magn. Mater. Magn.* **67** 65
[67] Skaftouros S, Özdoğan K, Şaşioğlu E and Galanakis I 2013 *Phys. Rev. B* **87** 024420
[68] Özdoğan K, Şaşioğlu E and Galanakis I 2013 *Appl. J. Phys.* **113** 193903
[69] Şaşioğlu E, Sandratskii L M and Bruno P 2005 *Phys. Rev. B* **72** 184415